Letter Vol. 47, No. 11 / 1 June 2022 / Optics Letters 2911

Optics Letters

Enhancement of Smith–Purcell radiation from cylindrical gratings by quasi-bound states in the continuum

Zhaofu Chen,* Mengmeng Jin, Leilei Mao, Xin Shi, Ningfeng Bai, and Xiaohan Sun

Research Center for Electronic Device and System Reliability, Southeast University, Nanjing 210096, China
**Corresponding author: chen.zhaofu@outlook.com*

Received 10 February 2022; revised 12 May 2022; accepted 13 May 2022; posted 16 May 2022; published 31 May 2022

Smith–Purcell radiation (SPR) is an important means of generating terahertz waves, and the enhancement of SPR is an attractive topic nowadays. Inspired by the phenomenon of special SPR, where the enhancement is achieved by using a high-duty-cycle grating, we describe a new, to the best of our knowledge, but more effective approach to this challenging problem. By deriving a simple analytical solution for the SPR from an annular electron beam passing through a cylindrical metallic grating, we show that the inverse structure, a low-duty-cycle grating can exhibit rather high SPR efficiencies in the presence of quasi-bound states in the continuum (quasi-BICs). The analytical prediction is supported by particle-in-cell simulations, which show that the quasi-BICs can enhance the superradiant SPR generated by a train of electron bunches by orders of magnitude. These results present an interesting mechanism for enhancing the SPR from metallic gratings, and may find applications in terahertz free-electron lasers.

https://doi.org/10.1364/OL.455763

Terahertz wave generation is one of the most promising technologies in scientific research, and terahertz waves have a wide range of applications in the fields of biomedicine, communication, materials science, and security inspection [1–3]. At present, the main terahertz sources include pumped molecular gas lasers, quantum cascade lasers, backward wave oscillators, and gyrotrons, but there remain limitations within them [4–6]. The Smith–Purcell radiation (SPR) excited by electrons moving along a grating surface, which was first observed by Smith and Purcell in 1953 [7], is a promising terahertz source [8–15]. In the past two decades, considerable effort has been made to study superradiant SPR, which uses electron bunches to generate coherent radiation [16–20]. This mechanism is undoubtedly attractive for generating terahertz waves, but the radiated power is still low, owing to its spontaneous nature [8]. Improving the radiation efficiency is necessary for its applications in communications, physics, and biology.

Recently, it has been shown that, using dielectric gratings, the upper limit for the amount of SPR that can be extracted from free electrons can be approached by using the high-Q resonances near bound states in the continuum (BICs), which are known as quasi-BICs [21–23]. A BIC can be considered as a resonance that lies inside the continuum but remains perfectly trapped without leakage [24,25]. Coupling of electrons with leaky quasi-BIC resonances provides a great opportunity to strengthen the SPR, but the application of dielectrics in high-power terahertz sources is still limited by the surface charging problem in practice [26]. In comparison, metal gratings have been approved to be applicable in vacuum electronics [27], but the effect of quasi-BICs on the SPR has not been revealed for such materials. Although previous studies have shown that the intensity of the special SPR (S-SPR) enabled by the presence of a high-duty-cycle metallic grating can be an order of magnitude higher than that of ordinary SPR (O-SPR) in specific directions [28,29], the efficiency of metallic gratings still needs further improvement for practical applications.

In this paper, we present the ability of quasi-BICs for the metallic grating to enhance SPR. For the convenience of future experiments, we focus on the coupling between a cylindrical grating and an annular electron beam, which enables high current densities without the space-charge effect of pencil beams and the edge effect of sheet beams. Using the mode matching theory, we demonstrate that the quasi-BICs can also be supported by cylindrical gratings. When the bunching frequency of a bunched electron beam matches the frequency of a quasi-BIC, the coherent SPR produced by the superradiant effect can be substantially enhanced. This study offers an effective method for developing terahertz sources.

Figure 1 shows the SPR produced by a cylindrical open metallic grating. The grating periodicity is denoted by p, the pillar width by b, the groove width by a, the inner radius by r_1 and the external radius by r_2. Consider a charged ring moving in the z direction at $r = r_b$ with the velocity $v_0 = \beta_0 c$ and the charge quantity q, where c is the speed of light. The current density can be expressed as $\boldsymbol{J}(r, z, t) = \widehat{z} q v_0 (2\pi r)^{-1} \delta(r - r_b)\delta(z - v_0 t)$. The current density in the frequency domain is then obtained via Fourier transform, as

$$\boldsymbol{J}(r, z, \omega) = \widehat{z} \frac{q\delta(r - r_b)}{2\pi r} e^{-ik_{z0}z}, \tag{1}$$

where $k_{z0} = k_0/\beta_0$ and $k_0 = \omega/c$ [30]. The incident evanescent field induced by the electron beam toward the grating can be

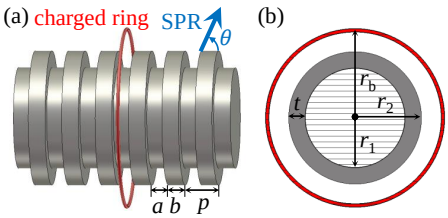

Fig. 1. (a) Smith–Purcell radiation from a cylindrical grating. (b) Transverse cross section of a cylindrical grating.

characterized by its azimuthal magnetic field:

$$H_{\varphi}^{\mathrm{in}}(r,z) = -\tau_0 \frac{q}{2\pi} K_0(\tau_0 r_b) I_1(\tau_0 r)\, \mathrm{e}^{-\mathrm{i}k_{z0}z}, \qquad r<r_{\mathrm{b}}, \tag{2}$$

where $\tau_0 = ({k_{z0}}^2 - k_0^2)^{1/2}$. The fields reflected by the periodic grating can be expressed in terms of space harmonics, with n being the diffraction order, R_n the reflection coefficient,

$$E_z^{\mathrm{re}}(r,z) = A\sum_{n=-\infty}^{\infty} R_n \frac{K_0(\tau_n r)}{K_0(\tau_n r_2)} \mathrm{e}^{-\mathrm{i}k_{zn}z}, \tag{3}$$

$$H_{\varphi}^{\mathrm{re}}(r,z) = -A\sum_{n=-\infty}^{\infty} \frac{\mathrm{i}\omega\varepsilon_0}{\tau_n} R_n \frac{K_1(\tau_n r)}{K_0(\tau_n r_2)} \mathrm{e}^{-\mathrm{i}k_{zn}z}, \tag{4}$$

where $k_{zn} = k_{z0} + 2n\pi/p$, $\tau_n = \left({k_{zn}}^2 - k_0^2\right)^{1/2}$, and

$$A = -\frac{\tau_0^2}{\mathrm{i}\omega\varepsilon_0}\frac{q}{2\pi} K_0(\tau_0 r_b) I_0(\tau_0 r_2). \tag{5}$$

Noticeably, for these radiating diffraction waves, with τ_n being imaginary, rewriting the z wavenumber k_{zn} in terms of the radiation angle θ_n yields the well-known relation between the radiation wavelength λ and the normalized electron velocity β_0:

$$\lambda = -\frac{p}{n}\left(\frac{1}{\beta_0} - \cos\theta_n\right). \tag{6}$$

The fields in the groove comprise a series of groove modes, with $m = 0, 1, 2$, etc., being the order and B_m being the coefficient of the mth order determined by the boundary conditions

$$E_z^{\mathrm{gv}}(r,z) = A\sum_{m=0}^{\infty} B_m \cos(k_{am}z) S_{0,m}, \tag{7}$$

$$H_{\varphi}^{\mathrm{gv}}(r,z) = A\sum_{m=0}^{\infty} \frac{\mathrm{j}\omega\varepsilon_0}{\zeta_m} B_m \cos(k_{am}z) S_{1,m}, \tag{8}$$

where

$$S_{0,m}(r) = K_0(\zeta_m r_1) I_0(\zeta_m r) - I_0(\zeta_m r_1) K_0(\zeta_m r), \tag{9}$$

$$S_{1,m}(r) = K_0(\zeta_m r_1) I_1(\zeta_m r) + I_0(\zeta_m r_1) K_1(\zeta_m r), \tag{10}$$

$$\zeta_m = \left[k_{am}^2 - k_0^2\right]^{1/2}, \qquad k_{am} = m\pi/a. \tag{11}$$

Here, m being even and odd corresponds to even-symmetric and odd-symmetric groove modes in the z direction, respectively.

Considering $M+1$ groove modes in the groove and $2N+1$ space harmonics for the reflected wave, the reflection matrix $\boldsymbol{R}$ can be derived by imposing the continuity of the boundary conditions at the grating surface [31],

$$\boldsymbol{R} = \left(\boldsymbol{E}^{\mathrm{T}}\boldsymbol{D}\boldsymbol{H}\boldsymbol{F} + \boldsymbol{I}\right)^{-1}\left(\boldsymbol{E}^{\mathrm{T}}\boldsymbol{D}\boldsymbol{H}\boldsymbol{G} - \boldsymbol{I}\right)\boldsymbol{L}, \tag{12}$$

where $\boldsymbol{I}$ is the identity matrix and

$$\boldsymbol{R} = [R_{-N}, R_{-N+1}, \ldots, R_N]^{\mathrm{T}} \in \mathbb{C}^{(2N+1)\times 1}, \tag{13}$$

$$\boldsymbol{D} = \mathrm{diag}\left[S_{0,m}(r_2)/S_{1,m}(r_2)\right] \in \mathbb{C}^{(M+1)\times(M+1)}, \tag{14}$$

$$\boldsymbol{F} = \mathrm{diag}\left[K_1(\tau_n r_2)/\tau_n K_0(\tau_n r_2)\right] \in \mathbb{C}^{(2N+1)\times(2N+1)}, \tag{15}$$

$$\boldsymbol{G} = \mathrm{diag}\left[I_1(\tau_n r_2)/\tau_n I_0(\tau_n r_2)\right] \in \mathbb{C}^{(2N+1)\times(2N+1)}, \tag{16}$$

$$\boldsymbol{L} = [0, \ldots, 0, 1, 0, \ldots, 0]^{\mathrm{T}} \in \mathbb{C}^{(2N+1)\times 1}, \tag{17}$$

$$H_{m,n} = \frac{2-\delta_{m,0}}{a}\zeta_m \int_0^a \mathrm{e}^{-\mathrm{i}k_{zn}z}\cos(k_{am}z)\,\mathrm{d}z, \tag{18}$$

$$E_{m,n} = \frac{1}{p}\int_0^a \mathrm{e}^{\mathrm{i}k_{zn}z}\cos(k_{am}z)\,\mathrm{d}z. \tag{19}$$

The coefficient B_m can be calculated by

$$\boldsymbol{B} = \boldsymbol{U}^{-1}\boldsymbol{H}(\boldsymbol{G}\boldsymbol{L} - \boldsymbol{F}\boldsymbol{R}), \tag{20}$$

where

$$\boldsymbol{B} = [B_0, B_1, \ldots, B_M]^{\mathrm{T}} \in \mathbb{C}^{(M+1)\times 1}, \tag{21}$$

$$\boldsymbol{U} = \mathrm{diag}\left[S_{1,m}(r_2)\right] \in \mathbb{C}^{(M+1)\times(M+1)}. \tag{22}$$

Here, $|R_{-n}|^2$, which is the efficiency factor and is independent of q and r_{b}, is the key parameter in the calculation [32].

Now we use this analytical method to show that the BICs also occur in the SPR from cylindrical gratings. Instead of high-duty-cycle gratings that have been extensively studied, we focus on low-duty-cycle gratings, which are less considered. In Fig. 2(a), we show the efficiency factor $|R_{-1}|^2$ calculated with $M = N = 25$ as a function of k_{z0} and SPR frequency f for grating period $p = 602.7$ μm, duty cycle $\eta = 0.1$, thickness $t = 3p$, external radius $r_2 = 6p$. Here, for a given k_{z0}, the SPR frequency f is determined by the normalized electron velocity β_0, i.e., $f = k_{z0}\beta_0 c/2\pi$. This figure is essentially a dispersion diagram, where the dispersion curves are indicated by the singularity of $|R_{-1}|^2$ caused by electromagnetic resonances [33]. The nth-order space harmonic being propagating in the r direction requires $|k_{zn}|<k_0$. The white and magenta dashed lines indicate the cutoff conditions for the −1st-order and −2nd-order reflected space harmonics, respectively. We focus on the radiation continuum located above the white dashed lines, where the −1st-order propagates as SPR.

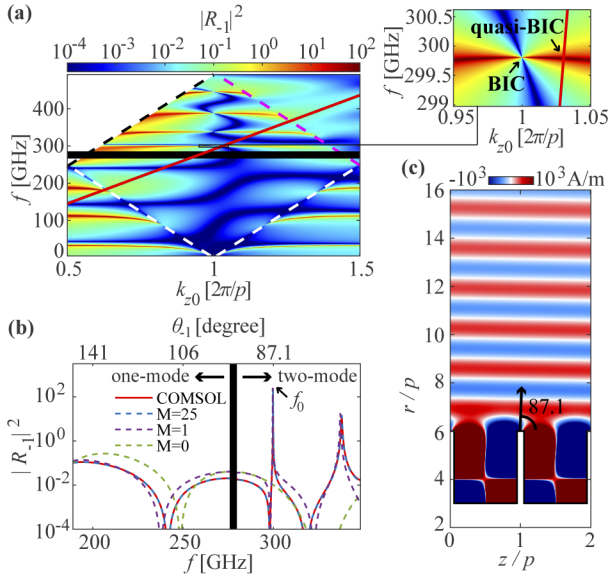

Fig. 2. SPR calculated by analytical solution. (a) f–k_{z0} maps of efficiency factor $|R_{-1}|^2$. (b) $|R_{-1}|^2$ versus radiation frequency f and angle θ_{-1} along the red solid line in (a), compared with COMSOL calculation. (c) H_{φ} field at the resonant frequency f_0 in (b).

Figure 2(a) shows that each resonance in the radiation continuum encounters a vanishing linewidth at $k_{z0} = 2\pi/p$. Such phenomenon indicates the existence of BICs, which are featured by an infinitely high quality factor embedded in the radiation continuum [24]. To find the causes of these BICs, the cutoff frequency of the second groove mode with $m = 1$ is indicated by the black solid line in Fig. 2(a). Considering that the BICs are all located above this line, we infer that they are directly related to the resonance of the second groove mode inside the grating groove. We also note that the identical k_{z0} of all these BICs corresponds to a special radiation angle $\theta_{-1} = 90°$, indicating the even-symmetry nature in the z direction of the SPR, which is in contrast to the odd-symmetry nature of the second groove mode. Consequently, the coupling of this odd groove mode to the even SPR at radiation angle $\theta_{-1} = 90°$ is forbidden by symmetry, leading to symmetry-protected BICs [24].

Although a perfect BIC is fully trapped, the high-Q quasi-BIC resonances near BICs are leaky and can offer an enhancement mechanism for SPR. As an example, we consider a normalized electron velocity $\beta_0 = 0.585$. The corresponding beam line is represented by the red solid line in Fig. 2(a), which intersects a strong resonance near the BIC, as indicated by the right inset. Figure 2(b) presents the $|R_{-1}|^2$ versus radiation frequency f and angle θ_{-1} along this red solid line calculated using COMSOL and the analytical solution with $M = 1, 2, 25$, and $N = 25$ [34]. It shows that the required value of M to ensure accuracy depends on the number of propagating groove modes, e.g., in the two-mode regime above the cutoff frequency of the second groove mode (the black solid line), $M + 1 = 2$ leads to a much better precision than $M + 1 = 1$. It also indicates that $M = N = 25$, used for Fig. 2(a), guarantees an excellent agreement between the analytical solution and COMSOL. The fact that there is no high-Q resonance in the analytical results with $M = 0$ is also evidence that supports our conjecture about the relationship between the BICs and the resonance of the second groove mode. At the resonant frequency of the quasi-BIC, $f_0 = 299.8$ GHz, the quality factor is found to be about 1.4×10^4 and the SPR efficiency can be enhanced by four orders of magnitude. By comparison, such enhancement is much more effective than the one-order-of-magnitude enhancement by S-SPR [28]. Figure 2(c) shows the H_φ field calculated by the analytical solution at the resonant frequency f_0, assuming $q = 1$. The radiation angle is 87.1°, in agreement with the value predicted by Eq. (6).

The capability of quasi-BIC resonance to enable such staggering enhancement of SPR at a specific direction has a great potential for the generation of coherent terahertz waves. As an example, we combine such a mechanism with the superradiant effect. Considering a continuous train of electron bunches, if the bunching frequency f_b or its higher harmonics are located in the radiation continuum, coherent SPR can be emitted, owing to the superradiant effect. Apparently, for the grating used in Fig. 2(b), when the bunching frequency of the electron beam or its higher harmonics approaches the frequency f_0, the superradiant SPR field can be enhanced by the quasi-BIC.

Now we show that the quasi-BIC can be utilized for the enhancement of superradiant SPR by performing the three-dimensional simulation with the particle-in-cell (PIC) code CST particle studio. As shown in Fig. 3(a), the electron energy and grating parameters follow those given in Fig. 2(b). The number of grating periods is set to be 41. The beam is set to be uniform in the r direction, with beam thickness $t_b = p/5$, the space between the beam and grating $d_b = p/10$. The current and

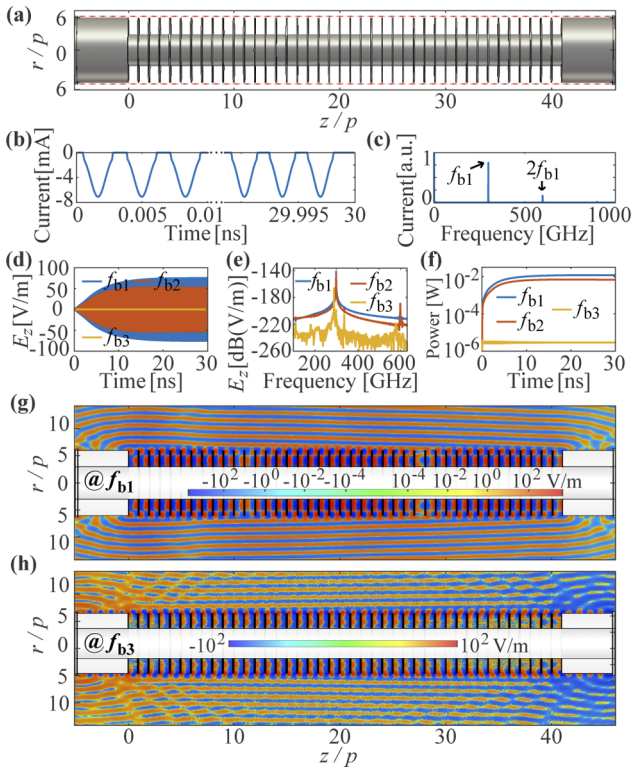

Fig. 3. Superradiant SPR calculated by PIC simulation. (a) Simulation model of the cylindrical grating driven by electron bunches. (b) Current and (c) spectrum of the electron beam with $f_b = f_{b1}$. (d)–(f) Detected (d) E_z fields, (e) spectrum, and (f) power for different bunching frequencies f_{b1}, f_{b2}, and f_{b3}. (g), (h) Contours of E_z field for (g) f_{b1} and (h) f_{b3}: $f_{b1} = 299.2$ GHz, $f_{b2} = f_{b1} + 10$ MHz, and $f_{b3} = f_{b1} - 10$ GHz.

spectrum of the electron beam, including both the fundamental bunching frequency and a series of high harmonics, are shown in Figs. 3(b) and 3(c), respectively. The current of these electron bunches follows the truncated Gaussian distribution and the linewidth at the bunching frequency is about 0.03 GHz, which is small in order to study the dependence of SPR power on the bunching frequency.

In the PIC simulation, the bunching frequency f_b of the electron beam is fine-tuned around f_0 while the number of elementary charges in a single bunch stays unchanged at 5.9×10^4, and the strongest SPR is found at $f_{b1} = 299.2$ GHz, which is roughly in agreement with the analytical solution. Figures 3(d) and 3(e) show the E_z fields above the grating and their spectra, respectively, with the bunching frequency f_{b1}, $f_{b2} = f_{b1} + 10$ MHz, and $f_{b3} = f_{b1} - 10$ GHz, detected at $z = 20p$ and $r = 12p$. The radiated power through a cylindrical face surrounding the whole structure at $r = 12p$ is presented in Fig. 3(f). The bunching frequency f_{b3} is sufficiently far away from the resonant frequency, so the corresponding SPR can be considered as the direct superradiant emission of the O-SPR. In comparison, the SPR power can be enhanced by more than three orders of magnitude with the bunching frequency f_{b1}, which demonstrates that the quasi-BICs can indeed substantially enhance the SPR. Such an enhancement factor is a little smaller than that in the analytical solution; this might be caused by the finite number of grating periods in the PIC simulation. Owing to the narrow linewidth of the incident fields from these electron bunches, the SPR linewidths for f_{b1},

f_{b2}, and f_{b3} remain 0.03 GHz. Here, we notice that, in the PIC simulation, the SPR fields saturate at different times, depending on the bunching frequency. This is because the analytical solution given by Eq. (12) is derived for the steady state, and the higher efficiency factor $|R_{-1}|^2$ near BICs essentially corresponds to a higher quality factor, which requires a longer saturation time in the PIC simulation. Figures 3(g) and 3(h) show the calculated E_z component for f_{b1} and f_{b3}, where the radiation angles are 87.1° and 90.6°, respectively, consistent with that predicted by Eq. (6). Noticeably, owing to the abrupt change of boundary, the resonant waves are scattered toward different angles at both ends of the grating [18].

The quasi-BICs provide an effective method to improve the efficiency of SPR sources and may greatly promote their practical use. Previous studies have shown that the existence of symmetry-protected BICs studied here is robust to small changes in the system [24], so the fabrication of such gratings is not over-challenging, considering its usage in vacuum electronics and quasi-BIC applications in terahertz [35,36]. Structurally, this concept also applies to planar gratings and various metamaterials supporting quasi-BICs [25]. The generation of electron bunches, which is essential for the experimental validation of the proposed superradiant SPR sources, can be obtained by using the self-induced interaction between a continuous electron beam and a surface wave [20], or by an external field, such as might be generated in a klystron [37]. Interestingly, the recent demonstration experiments of electron beam modulation by lasers provide feasible solutions for electron bunching in optics [38,39]. On this basis, the capability of quasi-BICs to enhance the SPR at harmonics of the bunching frequency might also be utilized for future optical radiation sources.

In summary, we show how to utilize the quasi-BICs of a low-duty-cycle cylindrical grating to improve the SPR efficiency. In the presence of a leaky resonance near the BIC, the SPR efficiency in the spontaneous regime can be greatly improved at a specific direction. Based on such a mechanism, using the resonant frequency as the bunching frequency of the electron beam, the coherent superradiant SPR from a train of electron bunches can be enhanced by orders of magnitude. This method may enable a powerful and coherent SPR source, which is useful for terahertz science and technology.

Funding. National Natural Science Foundation of China (61871110); National Key Laboratory of Science and Technology on Vacuum Electronics; Fundamental Research Funds for the Central Universities.

Disclosures. The authors declare no conflicts of interest.

Data availability. Data underlying the results presented in this paper are not publicly available at this time but may be obtained from the authors upon reasonable request.

REFERENCES

1. T. L. Cocker, V. Jelic, R. Hillenbrand, and F. A. Hegmann, Nat. Photonics **15**, 558 (2021).
2. J. Ma, R. Shrestha, J. Adelberg, C.-Y. Yeh, Z. Hossain, E. Knightly, J. M. Jornet, and D. M. Mittleman, Nature **563**, 89 (2018).
3. H. Matsumoto, I. Watanabe, A. Kasamatsu, and Y. Monnai, Nat. Electron. **3**, 122 (2020).
4. A. Khalatpour, A. K. Paulsen, C. Deimert, Z. R. Wasilewski, and Q. Hu, Nat. Photonics **15**, 16 (2021).
5. A. D. Koulouklidis, C. Gollner, V. Shumakova, V. Y. Fedorov, A. Pugžlys, A. Baltuška, and S. Tzortzakis, Nat. Commun. **11**, 292 (2020).
6. C. Paoloni, D. Gamzina, L. Himes, B. Popovic, R. Barchfeld, L. Yue, Y. Zheng, X. Tang, Y. Tang, P. Pan, H. Li, R. Letizia, M. Mineo, J. Feng, and N. C. Luhmann, IEEE Trans. Plasma Sci. **44**, 369 (2016).
7. S. J. Smith and E. M. Purcell, Phys. Rev. **92**, 1069 (1953).
8. V. L. Bratman, A. E. Fedotov, P. B. Makhalov, and F. S. Rusin, Appl. Phys. Lett. **94**, 061501 (2009).
9. E. A. Myasin, V. V. Evdokimov, and A. Y. Ilyin, Radiophys. Quantum Electron. **59**, 369 (2016).
10. D. I. Garaev, D. Y. Sergeeva, and A. A. Tishchenko, Phys. Rev. B **103**, 075403 (2021).
11. W. Liu, L. Sun, Z. Yu, B. Sun, and H. Xu, J. Appl. Phys. **127**, 184501 (2020).
12. Y. Ye, F. Liu, M. Wang, L. Tai, K. Cui, X. Feng, W. Zhang, and Y. Huang, Optica **6**, 592 (2019).
13. Z. Zhang, C. Du, J. Zhu, F. Han, F. Li, Z. Gao, L. Zhang, A. W. Cross, and P. Liu, J. Lightwave Technol. **39**, 6231 (2021).
14. T. Fu, D. Wang, Z. Yang, Z.-I. Deng, and W. Liu, Opt. Express **29**, 26983 (2021).
15. B. Hermann, U. Haeusler, G. Yadav, A. Kirchner, T. Feurer, C. Welsch, P. Hommelhoff, and R. Ischebeck, ACS Photonics **9**, 1143 (2022).
16. J. Urata, M. Goldstein, M. F. Kimmitt, A. Naumov, C. Platt, and J. E. Walsh, Phys. Rev. Lett. **80**, 516 (1998).
17. S. E. Korbly, A. S. Kesar, J. R. Sirigiri, and R. J. Temkin, Phys. Rev. Lett. **94**, 054803 (2005).
18. J. Gardelle, P. Modin, H. P. Bluem, R. H. Jackson, J. D. Jarvis, A. M. M. Todd, and J. T. Donohue, IEEE Trans. Terahertz Sci. Technol. **6**, 497 (2016).
19. A. Gover, R. Ianconescu, A. Friedman, C. Emma, N. Sudar, P. Musumeci, and C. Pellegrini, Rev. Mod. Phys. **91**, 035003 (2019).
20. L. Liang, W. Liu, Q. Jia, L. Wang, and Y. Lu, Phys. Plasmas **26**, 013102 (2019).
21. Y. Yang, A. Massuda, C. Roques-Carmes, S. E. Kooi, T. Christensen, S. G. Johnson, J. D. Joannopoulos, O. D. Miller, I. Kaminer, and M. Soljacic, Nat. Phys. **14**, 894 (2018).
22. Y. Song, N. Jiang, L. Liu, X. Hu, and J. Zi, Phys. Rev. Appl. **10**, 064026 (2018).
23. C. Roques-Carmes, S. E. Kooi, Y. Yang, A. Massuda, P. D. Keathley, A. Zaidi, Y. Yang, J. D. Joannopoulos, K. K. Berggren, I. Kaminer, and M. Soljacic, Nat. Commun. **10**, 3176 (2019).
24. C. W. Hsu, B. Zhen, A. D. Stone, J. D. Joannopoulos, and M. Soljacic, Nat. Rev. Mater. **1**, 16048 (2016).
25. K. Koshelev, S. Lepeshov, M. Liu, A. Bogdanov, and Y. Kivshar, Phys. Rev. Lett. **121**, 193903 (2018).
26. J. Breuer and P. Hommelhoff, Phys. Rev. Lett. **111**, 134803 (2013).
27. Y. Liang, Y. Du, D. Wang, L. Yan, Q. Tian, K. Chen, W. Huang, C. Tang, I. V. Konoplev, H. Zhang, and G. Doucas, Appl. Phys. Lett. **113**, 171104 (2018).
28. W. Liu and Z. Xu, New J. Phys. **16**, 073006 (2014).
29. W. Liu, L. Liang, Q. Jia, L. Wang, and Y. Lu, Phys. Rev. Appl. **10**, 034031 (2018).
30. P. M. van den Berg, J. Opt. Soc. Am. **63**, 689 (1973).
31. L. Schächter, *Beam-Wave Interaction in Periodic and Quasi-Periodic Structures* (Springer Science & Business Media, 2013).
32. P. M. van den Berg and T. H. Tan, J. Opt. Soc. Am. **64**, 325 (1974).
33. C. J. Chang-Hasnain and W. Yang, Adv. Opt. Photonics **4**, 379 (2012).
34. A. Szczepkowicz, L. Schächter, and R. J. England, Appl. Opt. **59**, 11146 (2020).
35. D. Gamzina, H. Li, L. Himes, R. Barchfeld, B. Popovic, P. Pan, R. Letizia, M. Mineo, J. Feng, C. Paoloni, and N. C. Luhmann, IEEE Trans. Nanotechnol. **15**, 85 (2016).
36. W. Zhang, A. Charous, M. Nagai, D. M. Mittleman, and R. Mendis, Opt. Express **26**, 13195 (2018).
37. H. Huang, Z. Chen, S. Li, H. He, H. Yuan, Z. Liu, and L. Lei, Phys. Plasmas **26**, 033107 (2019).
38. J. W. Henke, A. S. Raja, A. Feist, G. Huang, G. Arend, Y. Yang, F. J. Kappert, R. N. Wang, M. Möller, J. Pan, J. Liu, O. Kfir, C. Ropers, and T. J. Kippenberg, Nature **600**, 653 (2021).
39. R. Shiloh, J. Illmer, T. Chlouba, P. Yousefi, N. Schönenberger, U. Niedermayer, A. Mittelbach, and P. Hommelhoff, Nature **597**, 498 (2021).